

Evaluation of SrBr₂ Hydration Reaction Rate with Repeated Cycling

Takehiro Esaki*, Yuichi Sugai

Department of Earth Resources Engineering, Kyushu University, Fukuoka, Japan

Email: *esaki@mine.kyushu-u.ac.jp

How to cite this paper: Esaki, T. and Sugai, Y. (2022) Evaluation of SrBr₂ Hydration Reaction Rate with Repeated Cycling. *Journal of Materials Science and Chemical Engineering*, 10, 53-61.

<https://doi.org/10.4236/msce.2022.102005>

Received: November 17, 2017

Accepted: February 25, 2022

Published: February 28, 2022

Copyright © 2022 by author(s) and Scientific Research Publishing Inc.

This work is licensed under the Creative Commons Attribution International License (CC BY 4.0).

<http://creativecommons.org/licenses/by/4.0/>



Open Access

Abstract

In this study, we evaluated the SrBr₂ hydration reaction rate on repeated cycling. It was estimated that hydrated SrBr₂ particles were expanded by hydration and condensed to form secondary particles; thus, the hydration reaction was reduced by repeated cycles. Using volumetric methods, we examined the effect of repetition on the reaction rate for 900 cycles during hydration and dehydration and analyzed the reaction rate using the unreacted core-shell model. From the experimental and calculated results, we confirmed that reaction rate decreased and the sample particles formed secondary particles after 900 repeated cycles. By analyzing the unreacted core-shell model, we found that the coefficient of H₂O diffusion in the particles exponentially decreased with increasing repeated cycles. The value of the diffusion coefficient after 900 cycles was five times lower than that of the first cycle. To achieve stable repeated hydration cycles, technology to control the formation of secondary particles must be investigated.

Keywords

SrBr₂ Hydration, Repetition Cycle, The Coefficient of Particle Diffusion

1. Introduction

Chemical heat pump (CHP) technology utilizes exhaust heat. CHP can reduce the mismatch between supply and demand concerning the timing and grade of heat. For example, the cooling mode of CHP can generate cooling power for air conditioning, whereas the heat upgrading of CHP can increase heat temperature over the exhaust heat temperature. The amount of heat produced by CHP is higher than that produced by adsorption or absorption heat pumps using chemical reactions. Thus, the high heat density is an advantage in heat storage technology [1].

One problem affecting the practical application of CHP is the durability of the reversible reaction. Previous studies have suggested that the reaction system for CHP should be a pair of natural refrigerants (H_2O , NH_3 , or EtOH) and a hydro-oxide (CaO or MgO), a metal chloride (MgCl_2 , CaCl_2), or metal bromide (CaBr_2 , SrBr_2) [2] [3]. This reaction system is a gas-solid reaction system. These reaction systems undergo side reactions both before and after the reaction and chemical and physical changes, such as the expansion and contraction of reactants. Kato *et al.* studied the repeatability characteristics of the MgO hydration system by thermogravimetric analysis using a composite material comprising the reactant and expanded graphite [4]. This study revealed that composite materials had high durability concerning the repetition of the hydration reaction compared with pure MgO materials [5]. Ogura *et al.* evaluated the characteristics of the CaSO_4 hydration reaction on repeated cycling. This study revealed that ten repeated cycles had no effect on the reaction rate, but the reaction rate was decreased after 550 cycles [6]. The reason for this decrease was that during the hydration and dehydration reactions of CaSO_4 , irreversible chemical side reactions occurred. The change in the crystal structure of the reactants generated by side reactions was driven by the temperature conditions, and it was revealed the temperature conditions could be adjusted to maintain high reversibility. Kito *et al.* evaluated the heat output, and the repetition characteristics were suppressed below 10%. However, physical changes to the reactants occurred [7]. Kuwata *et al.* evaluated the repetition characteristics for the hydration of CaCl_2 in a plate tube heat exchanger [8]. The decrease in the reaction fraction was less than 10% in this reaction system, and reactor modules had a high durability of repetition. They investigated the reason for the decrease of reaction fraction, and it was found that the reactants particle were aggregated and removed from the reactor. In addition, the surface area of the reactants in the packed beds after the experiment was twice that before the experiment. It was revealed that the repetition reaction resulted in reactions and a change in the heat transfer characteristics.

In this study, we considered the SrBr_2 hydration reaction system. The SrBr_2 hydration reaction system has a high H_2O absorption capacity and a high heat storage density. Thus, this system was evaluated for the utilization of solar energy [9]. Previously, we investigated the hydration reaction characteristics using the unreacted core-shell model [10] [11]. And we calculated the activation energy of the hydration reaction and particle diffusion coefficient. Previously, Michel *et al.* have reported the characteristics of this system on repeated hydration/dehydration cycling [12]. The reaction rate was found to decrease over several repeated cycles. In this paper, the SrBr_2 hydration reaction characteristics over long-term repeated cycles were determined. We examined the effect of repetition on reaction rate for 900 cycles during hydration and dehydration by volumetric methods and analyzed reaction rate using the un-reacted core-shell model.

2. Experimental Procedure

Figure 1 shows a diagram of the experimental apparatus and SrBr₂ sample. In this experiment, the reaction characteristics were measured by the volumetric method. The experimental apparatus consisted of a reactor cell, a vapor tank, an evaporator, and a vacuum pump. Valves were connected between each unit. The vapor pressure was controlled by the evaporator and the vacuum pumps. The vapor pressure was controlled by the evaporator and the vacuum pumps. The vapor tank volume was 13 L. A pressure transducer (CCMT-100D) was set to measure the pressure change of the hydration and dehydration sample. The reactor cell was connected to the heating/cooling system by a thermostatic bath. The sample in the reactor cell was measured with a Pt resistance temperature sensor. The SrBr₂·6H₂O sample was obtained from Kanto Chemical, Inc., in Japan. The SrBr₂·6H₂O sample was dehydrated at 353 K, and the sample diameter was adjusted to 50 to 52 μm. In this experiment, the sample weight of SrBr₂ was set 10 mg to maintain a tank pressure change of less than 5%. **Table 1** shows the experimental conditions. In the repeated cycles, SrBr₂·6H₂O was generated by the hydration reaction, and the dehydrated SrBr₂ was generated by the vacuum pump. When the hydration reaction rate was measured over the repeated cycles, the tank vapor pressure was adjusted in order to obtain SrBr₂·H₂O, and the hydration reaction was analyzed using Equations (1) and (2).

$$\Delta P = \Delta n \frac{R_g T}{V_{\text{tank}}} \quad (1)$$

$$X = \frac{\Delta n_{\text{experiment}}}{n_{\text{theoretical}}} \quad (2)$$

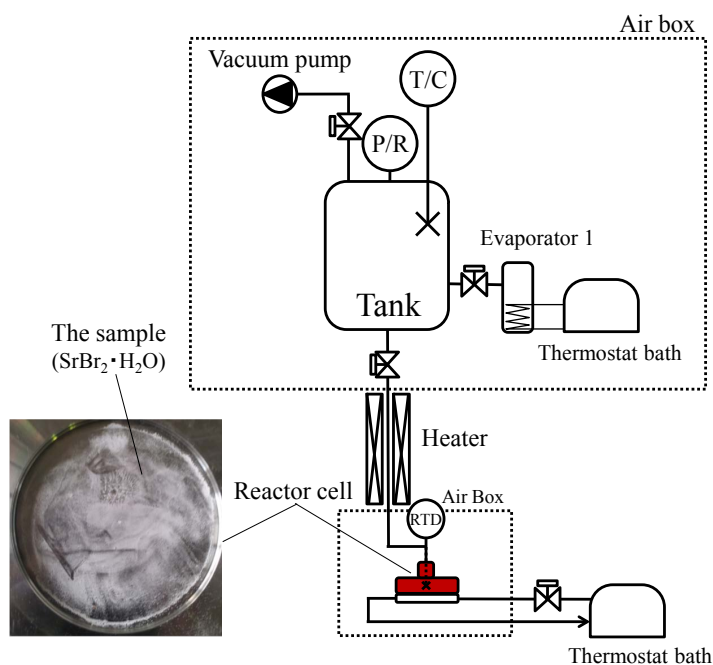


Figure 1. Schematic diagram of the experimental apparatus for the volumetric method.

Table 1. The experimental conditions.

	Repetition cycle		Measurement of reaction rate	
	Hydration	Dehydration	Hydration	Dehydration
Tank pressure [kPa]	1.3	0.01	1.23	0.6
Cell temperature [°C]	40	40	40	40
Change of hydration number	0 ⇒ 6	6 ⇒ 0	1 ⇒ 6	6 ⇒ 1

3. Reaction Rate Model

Solid-gas isothermal reaction models have been investigated using several mathematical models. **Figure 2** shows a schematic of the unreacted core-shell model for the solid-gas hydration reaction. Previously, we evaluated the SrBr₂ hydration reaction rate using the unreacted core-shell model. It has been shown that the reaction rate determining step is affected by the particle diameter. In this study, we expected the hydration reaction to be preceded by the particle intradiffusion rate step. The reaction rate can be written as in Equation (3).

$$-\gamma = \frac{dX}{dt} = \frac{3}{\rho R_s} \frac{R_s}{D_e} \left\{ (1-X)^{-1/3} - 1 \right\} \left(1 - \frac{P_e}{P} \right) \quad (3)$$

Equation (3) was obtained by integrating Equation (4).

$$f(X) = 1 - 3(1-X)^{2/3} + 2(1-X) = \frac{6D_e}{R_s^2} \left(1 - \frac{P_e}{P} \right) t \quad (4)$$

Equation (4) represents a function of the reaction fraction against time. The intraparticle diffusion coefficient was identified by numerical analysis of the temporal change of the reaction fraction based on experiment. In previous studies, the atomization of reactant particles or the palletization of reactant particles with expansion and contraction was caused by the repeated hydration and dehydration cycles. Thus, for the hydration reaction analysis model, the grain reaction model is more appropriate than the unreacted core-shell model. However, it is challenging to apply the grain reaction model to the hydration reaction because of the effects of diffusion resistance of single particle intradiffusion and the palletization of secondary particles. In this analysis, we assumed that the coefficient of intraparticle diffusion was changed with repeated cycling. The change in the diffusion resistance of the reactant with repeated cycling was standardized by the change in the intraparticle diffusion coefficient.

4. Experimental Results

Figure 3 shows the typical pressure variation of hydration with repeated cycles. The pressure of the tank decreased with increasing hydration, but the value of the pressure change was very small compared to the initial H₂O tank pressure. As shown in **Figure 3**, the decreased tank pressure rate changed with repeated cycling. The maximum reactant temperature change was 0.2°C over 900 cycles.

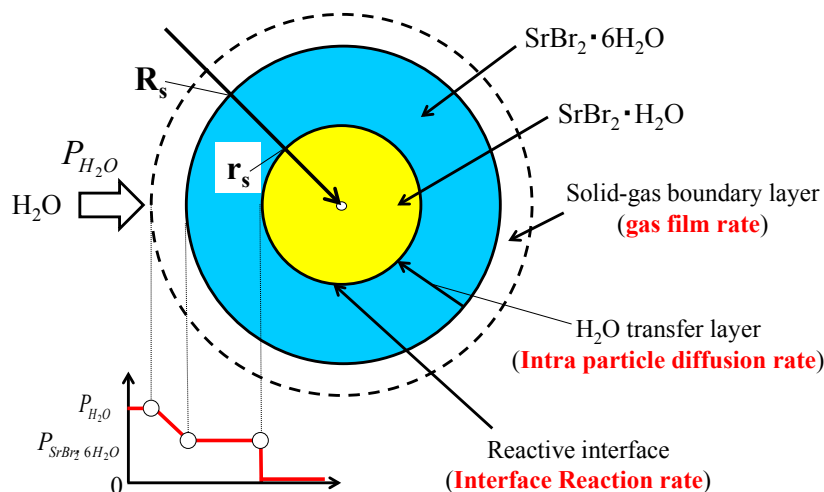


Figure 2. Schematic diagram of the unreacted-core shell model for the solid-gas hydration reaction.

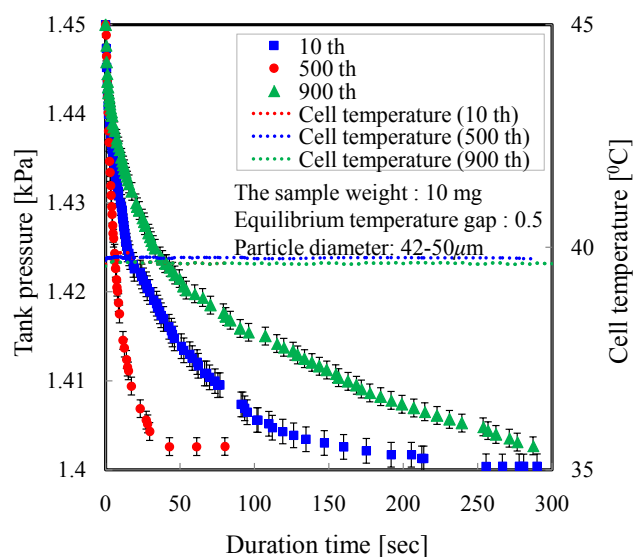


Figure 3. Typical variation in the tank pressure and cell temperature with time and repeated cycles.

The thermal resistance of the reactant was very low. Thus, the thermal resistance during repeated cycling was not affected by the hydration rate. **Figure 4** shows the reaction rate with increasing number of repeated cycles. After 10 cycles, the hydration reaction was completed within 50 s. On the other hand, those of 500 and 900 cycles were completed within 250 and 300 s, respectively. It can be noticed that the time for complete hydration increased. While, the hydration reaction rate decreased with increasing repeat cycle number. **Figure 5** shows a typical $f(X)$ plot reaching $X_{\text{react}} = 0.9$ for hydration over repeated cycles. The $f(X)$ plot for the intraparticle diffusion rate is fairly linear. The coefficient of intraparticle diffusion with repeated cycles was calculated from the slope of the $f(X)$ plots. **Figure 6** shows the coefficient of intraparticle diffusion with increasing repeated

cycles. **Table 2** summarizes the coefficients of intraparticle diffusion. From the results, we found that the resistance of H₂O diffusion increased as the number of repeated cycles increased. The value of the coefficient of diffusion after 10 cycles was ten times higher than that after 900 cycles. **Figure 7** shows a photograph of reactor cell after 900 cycles. The particle diameter had increased, and secondary particles had formed by condensation with each primary particle. For example, a secondary particle with a diameter of 1 mm was formed after repeated cycling (before repeated cycling: 42 - 50 μm). Therefore, we estimated that the H₂O diffusion resistance of the sample particles increased with increasing generation of secondary particles by repeated cycling.

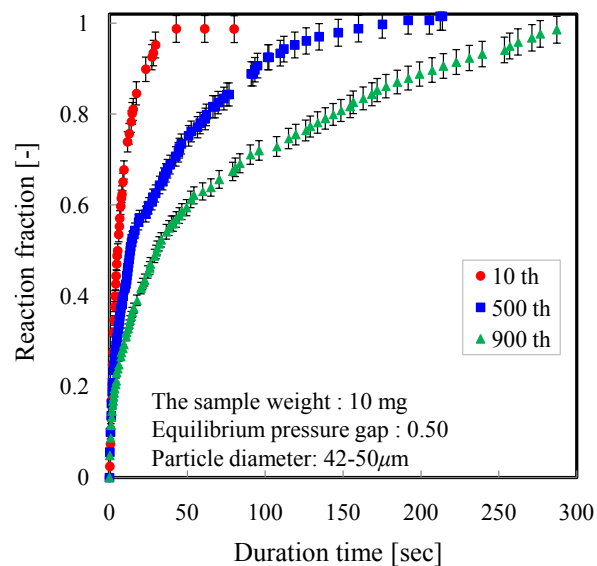


Figure 4. Typical variation in the reaction fraction with time and repeated cycles.

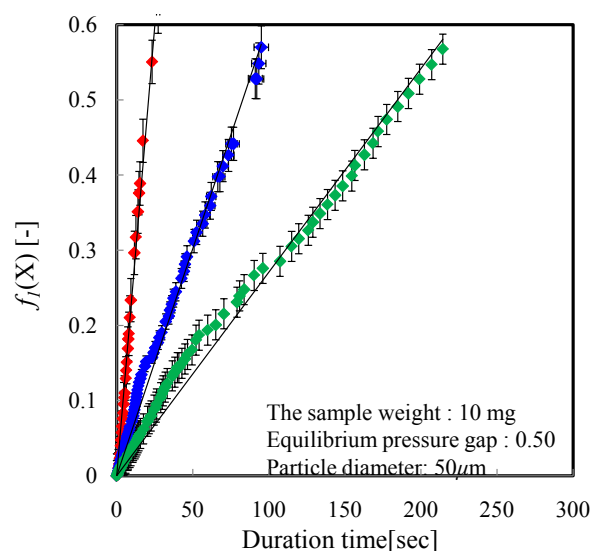


Figure 5. $f_i(X)$ plots reaching $X_{\text{react}} = 0.9$ for a particle diameter of 50 μm .

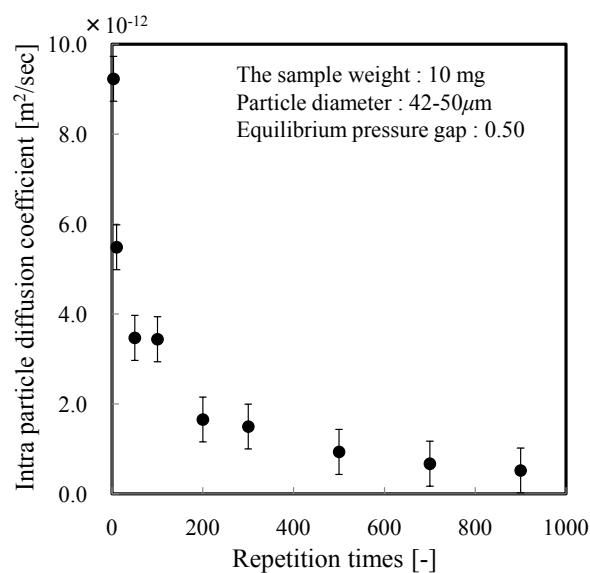


Figure 6. The coefficient of intraparticle diffusion with repeated cycles.



Figure 7. Photographs of the SrBr₂ sample before and after repeated cycles.

Table 2. The change of coefficient of particle diffusion with repeated cycles.

Cycle number	3	10	50	100	200	300	500	700	900	[-]
D_{eff}	9.23	5.49	3.47	3.44	1.65	1.49	0.93	0.67	0.52	$\times 10^{12}$ [m ² /s]

In the future, we will evaluate the secondary particle formation step of the hydration reaction and calculate the coefficient of secondary particle diffusion using the grain model. In addition, we will investigate control technology for the prevention of condensation during repeated cycling.

5. Conclusion

We evaluated the SrBr₂ hydration characteristics with repeated cycles by experiment. From the experimental results, we found that the SrBr₂ hydration reaction rate decreased with increasing repeated cycles. The SrBr₂ sample underwent condensation, resulting in the formation of secondary particles. The hydration rates

were analyzed using an unreacted core-shell model. The coefficient of intraparticle diffusion decreased with increasing repeated cycles as the diffusion resistance in the particles increased. In the future, we will evaluate the formation of the secondary particles and investigate control technology for the prevention of condensation during repeated cycling.

Conflicts of Interest

The authors declare no conflicts of interest regarding the publication of this paper.

References

- [1] Edem N'Tsoukpoe, K., Le Pierrès, N., Liu, H. and Luo, L. (2009) A Review of Long-Term Sorption Solar Energy Storage. *Renewable and Sustainable Energy Reviews*, **13**, 2385-2396. <https://doi.org/10.1016/j.rser.2009.05.008>
- [2] Kokouvi, E.N., Holger, U.R., Armand, F.L., Kathrin, K., Beatriz, A.W., Thomas, S. and Wolfgang, K.L.R. (2015) A Review on the Use of Calcium Chloride in Applied Thermal Engineering. *Applied Thermal Engineering*, **75**, 513-531. <https://doi.org/10.1016/j.applthermaleng.2014.09.047>
- [3] Lahmidi, H., Mauran, S. and Goetz, V. (2006) Definition, Test and Simulation of a Thermochemical Storage Process Adapted to Solar Thermal Systems. *Solar Energy*, **80**, 883-893. <https://doi.org/10.1016/j.solener.2005.01.014>
- [4] Kato, Y., Yamashita, N. and Yoshizawa, Y. (1993) Study of a Chemical Heat Pump with Reaction System of Magnesium Oxide/Water. *Kagaku Kogaku Ronbunshu*, **19**, 1213-1216.
- [5] Kato, Y., Kobayashi, K. and Yoshizawa, Y. (1998) Durability to the Repetitive Reaction of Magnesium Oxide/Water Reaction System for a Heat Pump. *Applied Thermal Engineering*, **18**, 85-92. [https://doi.org/10.1016/S1359-4311\(97\)00058-6](https://doi.org/10.1016/S1359-4311(97)00058-6)
- [6] Lee, J., Ogura, H. and Sato, S. (2014) Reaction Control of CaSO₄ during Hydration/Dehydration Repetition for Chemical Heat Pump System. *Applied Thermal Engineering*, **63**, 192-199. <https://doi.org/10.1016/j.applthermaleng.2013.10.043>
- [7] Kato, T. and Kobayashi, N. (2012) Output Characteristics Evaluation of Heat Upgrading Operation in a CaBr₂/H₂O Chemical Heat Pump. *Japan Society of Energy and Resources*, **33**, 1-8.
- [8] Kuwata, K., Esaki, T., Yasuda, M., Matsuda, T., Kobayashi, N., Shiren, Y. and Aman, Y. (2017) Durability of Thermochemical Heat Storage Demonstrated through Long-Term Repetitive CaCl₂/H₂O Reversible Reactions. *Journal of Renewable and Sustainable Energy*, **9**, 024102. <https://doi.org/10.1063/1.4978351>
- [9] Farcot, L., Pierrès, N.L. and Fourmigué, J.F. (2019) Experimental Investigation of a Moving-Bed Heat Storage Thermochemical Reactor with SrBr₂/H₂O Couple. *Journal of Energy Storage*, **26**, 101009. <https://doi.org/10.1016/j.est.2019.101009>
- [10] Esaki, T. and Kobayashi, N. (2016) Reaction Rate Characteristics of SrBr₂ Hydration System for a Chemical Heat Pump Cooling Mode. *Journal of Materials Science and Chemical Engineering*, **4**, 106-115. <https://doi.org/10.4236/msce.2016.42012>
- [11] Esaki, T., Kuwata, K., Ichinose, A. and Kobayashi, N. (2017) Reaction Rate Analysis with Unreacted-Core Shell Model for a Chemical Heat Pump Cooling Mode with SrBr₂ Hydration. *Transactions of the JSME*, **83**, 1-9. (In Japanese)
- [12] Michel, B., Mazet, N., Mauran, S., Stitou, D. and Xu, J. (2012) Thermochemical

Process for Seasonal Storage of Solar Energy: Characterization and Modeling of a High-Density Reactive Bed. *Energy*, **47**, 553-563.
<https://doi.org/10.1016/j.energy.2012.09.029>

Nomenclature

$f_{(X)}$	= fraction of Alenius plot	[-]
D_{eff}	= coefficient of diffusion	[m ² ·s ⁻¹]
n	= molecular	[mol]
P	= pressure	[kPa]
R_s	= particle diameter	[m]
R_g	= gas constant	[kJ·K ⁻¹ ·mol ⁻¹]
T	= temperature	[K]
t	= time	[s]
V	= volume	[m ³]
X	= reaction fraction	[-]
ρ	= density	[kg·m ⁻³]
γ	= reaction rate	[s ⁻¹]